THE ASTROPHYSICAL JOURNAL, 198:407–417, 1975 June 1

STELLAR EVOLUTION AT HIGH MASS WITH SEMICONVECTIVE MIXING ACCORDING TO THE LEDOUX CRITERION

RICHARD STOTHERS AND CHAO-WEN CHIN
Institute for Space Studies, Goddard Space Flight Center, NASA
Received 1974 November 4

ABSTRACT

Semiconvective mixing has been included in new evolutionary sequences of models for stars of 10, 15, and 30 $M_\odot$, with four different initial chemical compositions. The models have been constructed with the help of the Ledoux criterion both for the definition of convective instability and for the state of convective neutrality that is assumed to be attained in regions with a gradient of mean molecular weight. Allowance for convective overshooting has also been made. Semiconvection is found to be almost nonexistent at 10 $M_\odot$ and of minor importance at 15 $M_\odot$. But at 30 $M_\odot$ semiconvection covers most of the intermediate zone and develops into full convection if the initial hydrogen and metals abundances are both high. If the initial metals abundance is low, a "blue loop" phase follows the early red-supergiant phase during core helium burning, just as it does for all initial chemical compositions at 10 and 15 $M_\odot$, when the new 3α reaction rate is adopted. If the initial hydrogen abundance is low, the star goes directly into a "blue hook" phase without first becoming a red supergiant. The critical importance of the depths of the semiconvective zone and of the outer convective envelope in promoting a blue loop and in determining the maximum effective temperature attained on the loop is demonstrated. The thermally stable stages of the blue-loop phase cover an amount of log T_e and a fraction of the helium-burning lifetime that are almost independent of stellar mass, although the maximum effective temperature attained on the loop is hotter at higher stellar masses. The effective temperature ranges agree roughly with observational data, but the predicted blue-to-red ratios for masses higher than about 15 $M_\odot$ do not.

Subject headings: convection — interiors, stellar — luminous stars — massive stars — stellar evolution

I. INTRODUCTION

When the Ledoux criterion for convective instability (Ledoux 1947; Sakashita, Ono, and Hayashi 1959) is used in models of massive stars, some ambiguity arises regarding the treatment of convectively unstable layers that contain a gradient of mean molecular weight. We showed in an earlier paper that a reasonable procedure is to leave these layers unmixed; the star then evolves into a red supergiant during the earliest stages of core helium depletion (Stothers and Chin 1968, Paper I). The only resulting modification of the chemical profile above the hydrogen-burning shell is the homogenization produced in layers covered by the outer convective envelope. It is sufficient (but not necessary) that the burning shell come close to the hydrogen-helium discontinuity at the base of the homogeneous region in order to induce the star subsequently to evolve into a blue supergiant (Stothers and Chin 1973, Paper II). Other authors (see Table 1 of Paper II) have verified at least the sufficiency of this condition in producing such a "blue loop"; more recent work is summarized in the present Table 1.

Originally, we thought that the modifications induced by semiconvective mixing in the intermediate zone of varying hydrogen-helium content were not likely to affect the overall evolution of the star. Although this has been amply verified for stages of evolution up to the onset of core helium burning, only four detailed evolutionary sequences including semiconvective mixing (15 $M_\odot$ [Robertson 1972]; 16 $M_\odot$ [Varshavsky 1972]; 20 $M_\odot$ [Chiosi and Summa 1970];

TABLE 1

FURTHER EVOLUTIONARY SEQUENCES OF MODELS FOR MASSIVE STARS BASED ON THE LEDOUX CRITERION*

$M/M_\odot$	X_e	Z_e	$\theta_\alpha{}^2$	$\epsilon_{3\alpha}$	log T_e (tip)	τ_b/τ_{He}	Author
10†.....	0.739	0.021	0.100	Old	4.04	0.4	Sackmann 1971
15.....	0.700	0.030	0.085	New	4.26	0.5	Ziołkowski 1972
16.....	0.602	0.044	~0.1	New	...	0.0	Varshavsky 1972, 1973
30.....	0.700	0.030	0.085	New	4.38	0.5	Ziołkowski 1972
32.....	0.602	0.044	~0.1	New	...	0.0	Varshavsky and Tutukov 1973
60.....	0.700	0.030	0.085	New	...	0.0	Ziołkowski 1972
64.....	0.602	0.044	~0.1	New	...	0.0	Varshavsky and Tutukov 1973

* Continuation of Tables 1 and 2 in Paper II.

† The Schwarzschild criterion was adopted for this sequence, but no mixing was allowed to occur in the intermediate zone; it was found that log T_e(tip) = 3.98 when the Watson, rather than the Cox-Stewart, opacities were used. Further sequences have been published (Sackmann 1974).

20 $M_\odot$ [Robertson 1972]) exist to indicate that this may also be true for the later stages as well. On the other hand, we have recently found that rather small changes in the physical input parameters of the models constructed without semiconvection can sometimes greatly influence the occurrence of the blue loop on the H-R diagram (Paper II). This remarkable sensitivity of the models has led us to reconsider, in this paper, the effect of including semiconvection in the models, for a broad range of masses and initial chemical compositions.

II. SEMICONVECTION

Mixing of material in regions containing a gradient of mean molecular weight was not permitted in Paper II even if the Ledoux criterion indicated convective instability (except that we did allow for downward penetration by the outer convective envelope). However, we found that convective instability develops at a mass fraction just above the former boundary of the zero-age convective core during the late stages of core hydrogen burning. The instability soon disappears, but later reappears (if the opacity is high enough) just below this boundary for a brief period during the early stages of core helium burning. Neglect of composition mixing during the first appearance of convective instability is certainly justified if convective overshooting from the unstable, chemically homogeneous layers is negligible. (But note that, despite the throttling effect on convection of a gradient of mean molecular weight, the outer convective envelope penetrating downward from the surface always manages to cover most of the previously inhomogeneous layers.) During the second appearance of convective instability near the former boundary of the zero-age core, the neglect of mixing may also be justified if the amount of mass involved is small.

The actual inclusion of mixing by convective overshooting in well-evolved stellar models was first studied about a decade ago for a star of 30 $M_\odot$ (Stothers 1966). The Ledoux criterion was adopted both for the definition of convective instability and for the state of convective neutrality (semiconvection) that was assumed to hold in unstable regions with a gradient of mean molecular weight (Sakashita and Hayashi 1961). The work of Sakashita and Hayashi had already established that the semiconvective zone originates around the boundary of the zero-age convective core, and then grows outward (and inward by overshooting) while remaining detached from the shrinking convective core. In the sequence for 30 $M_\odot$, a fully convective intermediate zone developed at the base of the semiconvective zone very late in the evolution, when helium was almost exhausted at the stellar center.

In the present work, we shall follow the prescription adopted earlier (Stothers 1966), with the exception that here, whenever a fully convective zone develops at the base of the semiconvective zone, the finite velocity of convective elements at the interface between the two zones is assumed to prevent the establishment of any chemical discontinuity there. However, the steep hydrogen gradient at the interface between the semiconvective zone (or the fully convective zone) and the underlying, strongly radiative zone is adequately approximated by a chemical discontinuity. Adaptation of the details of Ledoux-type semiconvective mixing to automatic numerical-relaxation programs has been made by a number of authors (Chiosi and Summa 1970; Robertson 1972; Varshavsky 1972); our own approach is rather similar to that of Robertson. Particular care has been taken to locate as accurately as possible the boundaries of the semiconvective and convective zones, by ensuring that (1) the exact opacity is used at all mesh points during each iteration to find a new model, (2) the radiative (or modified adiabatic) temperature gradient is employed during each iteration in the semiconvective layers, (3) not too much new mixing is allowed per time step, and (4) hydrogen is exactly conserved outside of the nuclear-burning regions. A lack of sufficient care in these matters can result in the development of spurious fully convective zones. In our program, we have proceeded by mixing the material after (not during) the iterations for a new model; then, with the new chemical profile, the model is relaxed again to check the consistency between the temperature gradient, the chemical profile, and the semiconvective (and fully convective) zonal boundaries; this process is repeated until a fully consistent solution is obtained. We have found that any reasonable choices for the distribution of mesh points and time steps yield nearly the same final results, as would be hoped for.

In terms of the nomenclature adopted earlier (Stothers 1970), our prescription for the intermediate zone in Paper II was essentially scheme R. The present prescription for the semiconvective zone alone is scheme M1, while that for the semiconvective zone underlain by a fully developed convective zone is scheme N1, modified by the allowance for convective overshooting between the two zones.

III. EVOLUTIONARY SEQUENCES WITH SEMICONVECTIVE MIXING ACCORDING TO THE LEDOUX CRITERION

New evolutionary sequences of stellar models with masses of 10, 15, and 30 $M_\odot$ have been calculated by use of the automatic computer program described in Paper II, but modified here to include mixing in the convectively unstable intermediate zones, as discussed in § II. Table 2 contains the main results, and is in the format of the corresponding Table 2 of Paper II. As before, we define: X_e, the initial hydrogen abundance by mass; Z_e, the initial metals abundance by mass; θ_α^2, the reduced α-particle width of the 7.12-MeV level in ^{16}O; and $\epsilon_{3\alpha}$, the rate of nuclear energy generation from the 3α process ("old" rate, Clayton 1968; "new" rate, Austin, Trentelman, and Kashy 1971). The Cox-Stewart opacities have again been used. For the convective envelopes we have adopted the "unmodified" low-temperature opacities and a ratio of mixing length to density scale height equal to 0.4. The output quantities in Table 2 include: the logarithm of the

TABLE 2

NEW EVOLUTIONARY SEQUENCES OF MODELS FOR STARS OF 10, 15, AND 30 $M_\odot$ BASED ON THE LEDOUX CRITERION WITH SEMICONVECTIVE MIXING*

Sequence	X_e	Z_e	$\theta_\alpha{}^2$	$\epsilon_{3\alpha}$	log T_e (tip)	τ_H (10^6 yr)	τ_{He}/τ_H	$\tau_b{}^{(1)}/\tau_{He}$	$\tau_b{}^{(2)}/\tau_{He}$	$\tau_y{}^{(1)}/\tau_{He}$	$\tau_y{}^{(2)}/\tau_{He}$
10-A	0.739	0.021	0.1	New	4.18	21.141	0.147	0.045	0.444	0.006	0.016
10-B	0.739	0.044	0.1	New	4.13	24.000	0.157	0.045	0.639	0.006	0.024
10-C	0.602	0.021	0.1	New	4.18	12.265	0.165	0.043	0.529	0.003	0.009
10-D	0.602	0.044	0.1	New	4.13	13.545	0.186	0.037	0.642	0.004	0.016
15-A	0.739	0.021	0.1	New	4.27	11.850	0.100	0.040	0.394	0.008	0.022
15-B	0.739	0.044	0.1	New	4.23	12.766	0.098	0.029	0.543	0.008	0.027
15-C	0.602	0.021	0.1	New	4.29	7.296	0.129	0.031	0.588	0.006	0.016
15-D	0.602	0.044	0.1	New	4.23	7.805	0.123	0.029	0.442	0.006	0.026
30-A	0.739	0.021	0.1	New	4.32	5.763	0.088	0.030	0.558	0.008	0.014
30-B	0.739	0.021	0.1	Old	...	5.763	0.083	0.036	...	0.010	...
30-C	0.739	0.044	0.1	New	...	5.988	0.084	0.028	...	0.006	...
30-D	0.602	0.021	0.1	New	4.16†	3.869	0.120	0.092	0.805†	0.013†	...
30-E	0.602	0.021	0.1	Old	4.16†	3.869	0.115	0.070	0.829†	0.011†	...
30-F	0.602	0.044	0.1	New	...	4.010	0.112	0.029	...	0.007	...
30-G	0.602	0.044	1.0	New	...	4.010	0.116	0.028	...	0.007	...
30-H	0.602	0.044	0.1	Old	...	4.010	0.108	0.032	...	0.007	...

* $\alpha = 0.4$ and "unmodified" opacities in the outer convective envelope.

† This sequence had no red-supergiant phase before the "blue loop," so that the first and second blue-supergiant phases were consecutive; the yellow-supergiant phase began later, when log $T_e = 3.85$.

effective temperature at the tip of the blue loop (if any); the lifetime of core hydrogen burning; the ratio of lifetimes of core helium burning and core hydrogen burning; and the fractions of time spent during core helium burning in the first and second blue (b) and yellow (y) supergiant configurations. All the sequences have been terminated at the end of core helium burning.

A general description of evolution in massive stars has already been given in Paper II. We recall that the depth of the convective envelope at the tip of the red-supergiant branch is a crucial factor, in many sequences, in determining whether or not a blue loop later occurs. The convective envelope becomes relatively deep, and hence a blue loop is more likely, if the opacity at the base of the envelope is high (e.g., if Z_e is high) or if the luminosity is high (e.g., if the new 3α rate is adopted). When a blue loop develops, the maximum effective temperature achieved is hotter if the new 3α rate is adopted, because the envelope is then more nearly uniform in chemical composition. This would also be true if a high value of Z_e were adopted, were it not for the fact that a high metals opacity tends also to expand the star and therefore counteracts the effect of envelope homogenization.

The various reasons for the slow blueward evolution along the loop and for the eventual termination of the loop have been explored elsewhere (Stothers 1966; Paper I). To summarize briefly: the outward burning of the hydrogen shell reduces the mass of the envelope by adding helium to the core; the structure of the star thus shifts toward that of a chemically homogeneous star, and therefore the effective temperature of the star gradually increases. When the shell has burned out to layers so hydrogen-rich that further growth is very slow, the chemical profile of the envelope is essentially frozen in, and the radius subsequently begins to expand, as it would for an ordinary main-sequence star. The very rich layers can be encountered either gradually, as when the intermediate zone into which the shell is burning possesses a smooth gradient of hydrogen, or else suddenly, as when the burning shell runs into the hydrogen discontinuity at the base of what was formerly the outer convection zone.

In the present paper, we shall concentrate on the evolutionary changes arising from semiconvective mixing, by making a comparison of the present sequences with the sequences calculated without it in Paper II.

a) Investigation of 10 $M_\odot$

The lowest mass at which semiconvection occurs on the main sequence is 8–10 $M_\odot$, depending on the adopted initial chemical composition and opacity source (Schwarzschild and Härm 1958; Percy 1970; Robertson 1972; Stothers 1972; Sreenivasan and Ziebarth 1974). In our present models for 10 $M_\odot$, the semiconvective zone develops for a brief period around the time of hydrogen exhaustion at the stellar center, while the star is at the most luminous part of the S-bend on the H-R diagram. Semiconvection covers a very small region near the former boundary of the zero-age convective core, and alters the chemical profile there by a trivial amount. Its effect on the subsequent evolution of the star is negligible.

Stellar evolution at 10 $M_\odot$ is, in fact, very much like that described in Paper II for the "non-semiconvective" sequences at 15 $M_\odot$. In particular, adoption of the new 3α rate ensures that a blue loop develops for all the adopted initial chemical compositions. Paczynski's (1970) sequence at 10 $M_\odot$ agrees quite well with our results, except that the tip of the blue loop is slightly cooler in his sequence. Although Sackmann

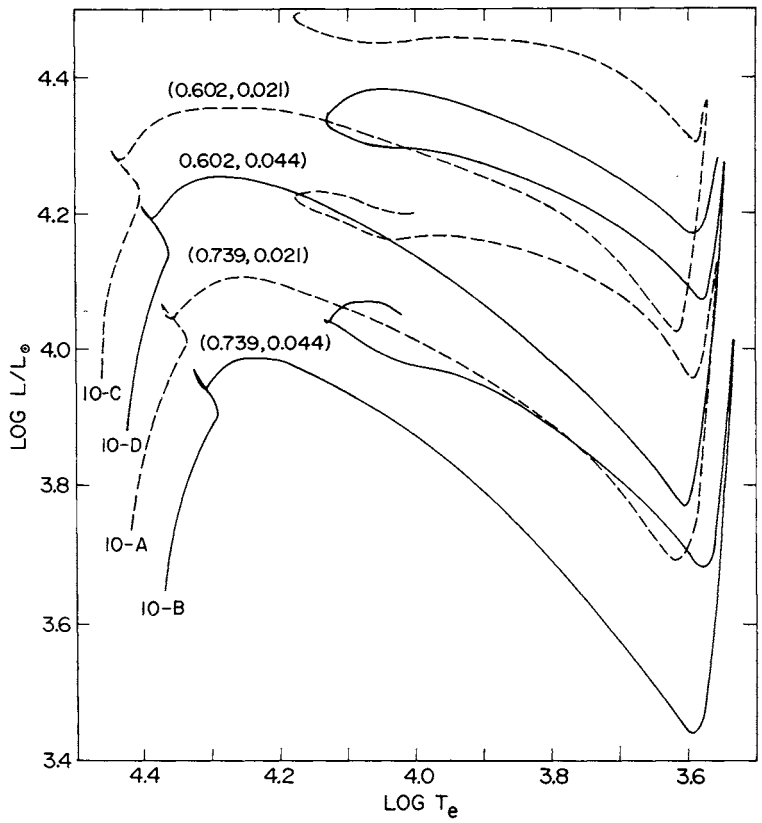

FIG. 1.—Theoretical evolutionary tracks in the H-R diagram for stars of 10 $M_\odot$. Tracks are labeled with (X_e, Z_e).

(1971) adopted the Schwarzschild criterion for convective instability, she assumed no mixing in the intermediate zone, and therefore her sequence at 10 $M_\odot$ is properly comparable with ours; her sequence is also somewhat cooler at the blue tip, as expected since she and Paczynski used the old 3α rate. Evolutionary tracks on the H-R diagram are shown for our models in Figure 1; the internal structural changes are displayed, for one chemical composition, in Figure 2.

b) Investigation of 15 $M_\odot$

Semiconvection at 15 $M_\odot$ breaks out around the former boundary of the zero-age convective core shortly before the instant of central hydrogen exhaustion, when the star is temporarily very bright.[1] Since the convective instability at this mass is stronger than at 10 $M_\odot$, it penetrates relatively farther into the layers having a gradient of mean molecular weight. The mixing motions raise the hydrogen content of the deeper layers by transporting hydrogen down from the outer layers; thus the hydrogen profile in the outer part of the intermediate zone tends to become rounded. The instability disappears not long after hydrogen vanishes at the center, as the star fades in brightness. If $Z_e = 0.044$, the high metals opacity causes part of the semiconvective zone to be reactivated temporarily when the star crosses the Hertzsprung gap. Although the semiconvective modifications at 15 $M_\odot$ are rather small, their effect on the subsequent evolution is noticeable, at least for $Z_e = 0.021$. The raised hydrogen content in the deeper layers of the semiconvective zone increases the opacity and lowers the gradient of mean molecular weight. Both factors drive deeper the strong convection originating at the stellar surface when the star becomes a red supergiant. In fact, the former semiconvective zone becomes totally immersed in the outer convection zone, so that memory of its structural history is eventually obliterated. But its influence has certainly been felt. The greater induced homogenization of the envelope means an earlier and a longer blue loop than was the case in Paper II. However, if $Z_e = 0.044$, the effect of the high metals opacity is so great that the semiconvective effects are unimportant in comparison, and therefore the corresponding sequences here and in Paper II are not significantly different from each other. Evolutionary tracks and structural changes are shown for some of our sequences in Figures 3, 4, and 5.

Agreement between the main features of Robertson's (1972) sequence for 15 $M_\odot$ and our corresponding sequence is found to be excellent. Although

[1] The small systematic difference of 2–3 percent in hydrogen-burning lifetime between the sequences calculated here and in Paper II is due to our present use of smaller time steps and more closely spaced mass zones.

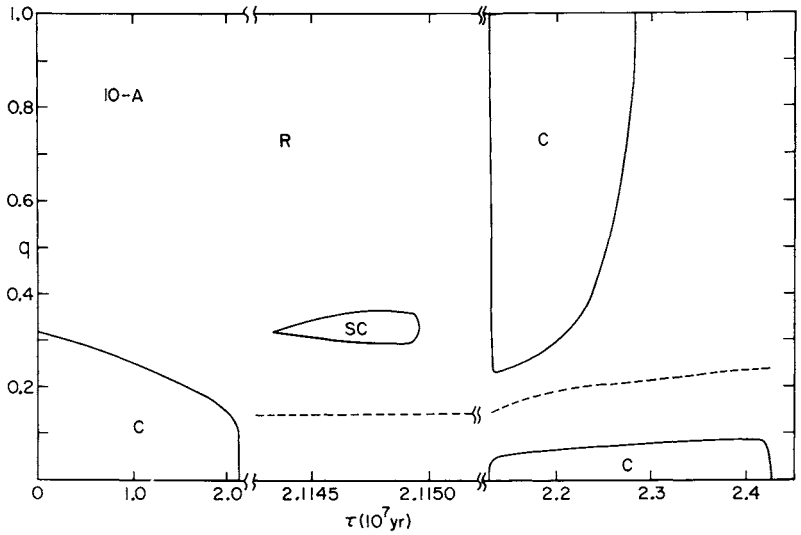

FIG. 2.—Evolution of the structural zones of a star of 10 $M_\odot$ with $(X_e, Z_e) = (0.739, 0.021)$. Coding is as follows: R, radiative; C, convective; SC, semiconvective. The dashed line represents the peak of the hydrogen-burning shell. The ordinate is mass fraction q. The abscissa, time, is divided into three segments, representing the following three phases of evolution: (1) core hydrogen burning, (2) transitional stages, and (3) core helium burning.

Ziołkowski (1972) did not include semiconvective mixing in his models, his sequence at 15 $M_\odot$ is also in good agreement with ours. This is not surprising, since the differences between our sequences with and without semiconvection are not very great. Varshavsky (1972, 1973) did not obtain a blue loop for his sequence at 16 $M_\odot$, probably because his treatment of surface convection resulted in a shallower convective envelope than the one obtained by Robertson, Ziołkowski, and us. In this connection, Paczynski (1970) seems to have been the first author to notice, by comparing two different sequences at 15 $M_\odot$, the crucial effect of small changes of the convective-envelope depth on the occurrence of blue loops.

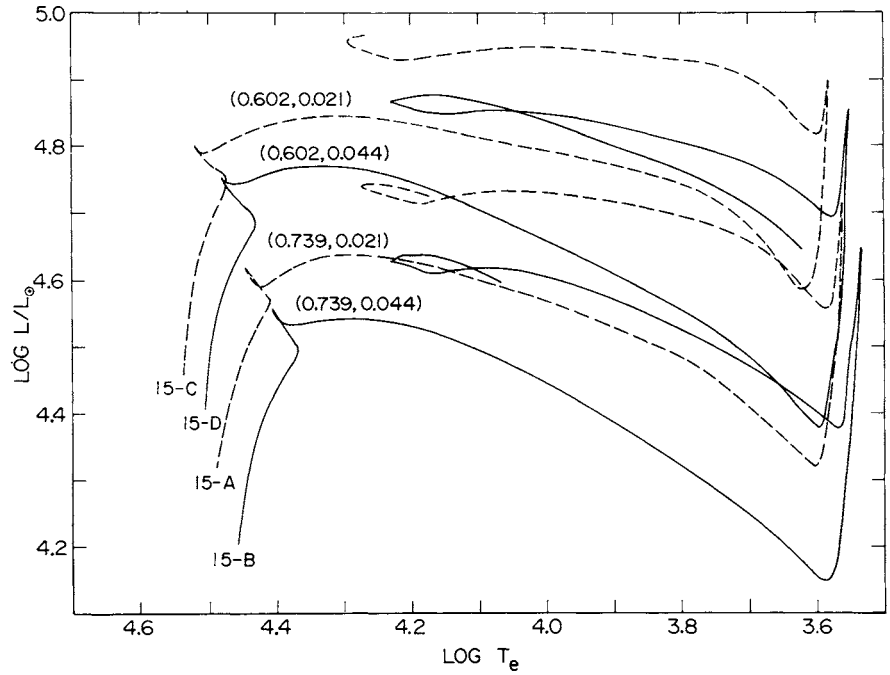

FIG. 3.—Theoretical evolutionary tracks in the H-R diagram for stars of 15 $M_\odot$. Tracks are labeled with (X_e, Z_e).

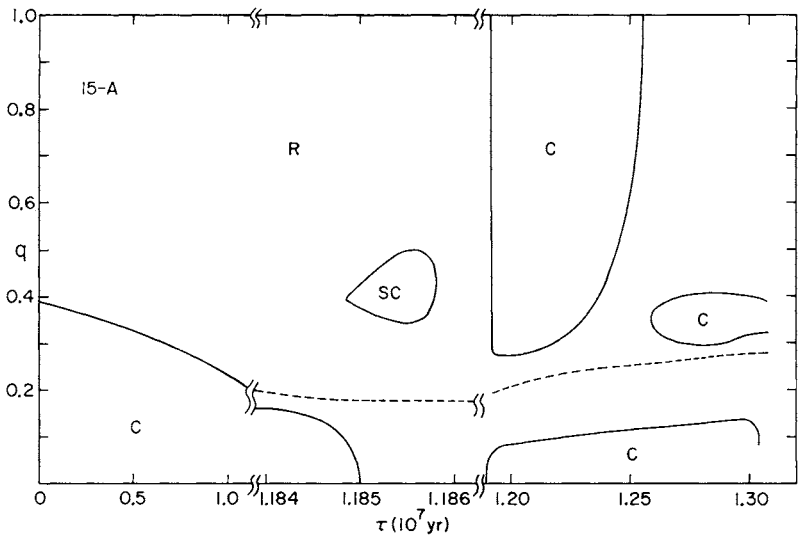

FIG. 4.—Evolution of the structural zones of a star of 15 $M_\odot$ with $(X_e, Z_e) = (0.739, 0.021)$. Coding is the same as in Fig. 2.

c) *Investigation of 30 $M_\odot$*

By far the most interesting results have been obtained for 30 $M_\odot$. At this mass the semiconvective zone develops during the main phase of core hydrogen burning, the exact stage of initial development being relatively late if the luminosity is low (i.e., if X_e is high). The subsequent evolution is extremely sensitive to the adopted initial chemical composition (see Fig. 6). Therefore, the present models in some cases differ drastically from those in Paper II, where the star remained a red supergiant throughout the phase of core helium burning for all choices of physical input parameters (see also Simpson 1971; Varshavsky and Tutukov 1973).

For $(X_e, Z_e) = (0.739, 0.021)$ the semiconvective zone disappears when $\log T_e = 4.29$. Since the metals opacity is small, semiconvection is never thereafter reactivated (see Fig. 7). The elevated hydrogen content in the former semiconvective zone eventually causes

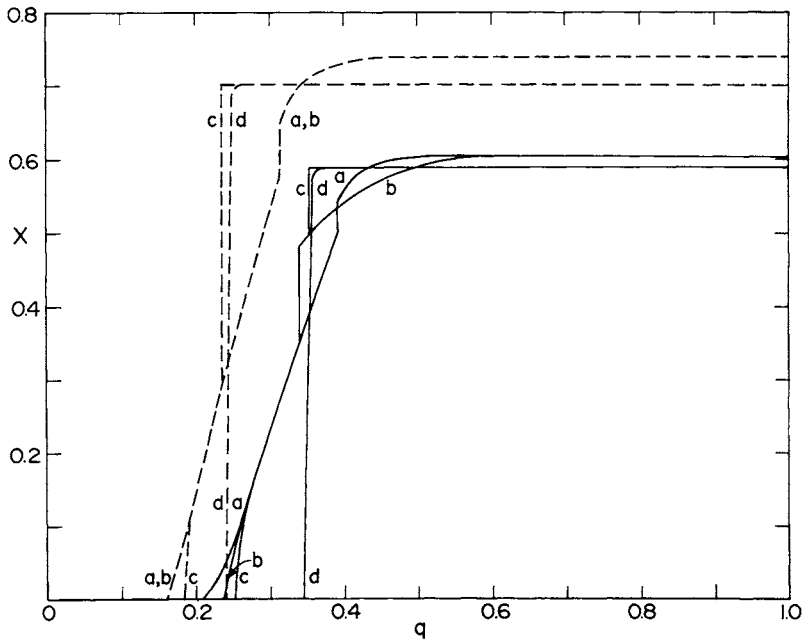

FIG. 5.—Hydrogen profiles for stellar models of 15 $M_\odot$ with $Z_e = 0.021$ (*solid lines*, sequence 15-C) and $Z_e = 0.044$ (*dashed lines*, sequence 15-B). Lettering index: *a*, end of core hydrogen burning; *b*, maximum extent of semiconvective zone; *c*, tip of the red-supergiant branch; and *d*, end of core helium burning.

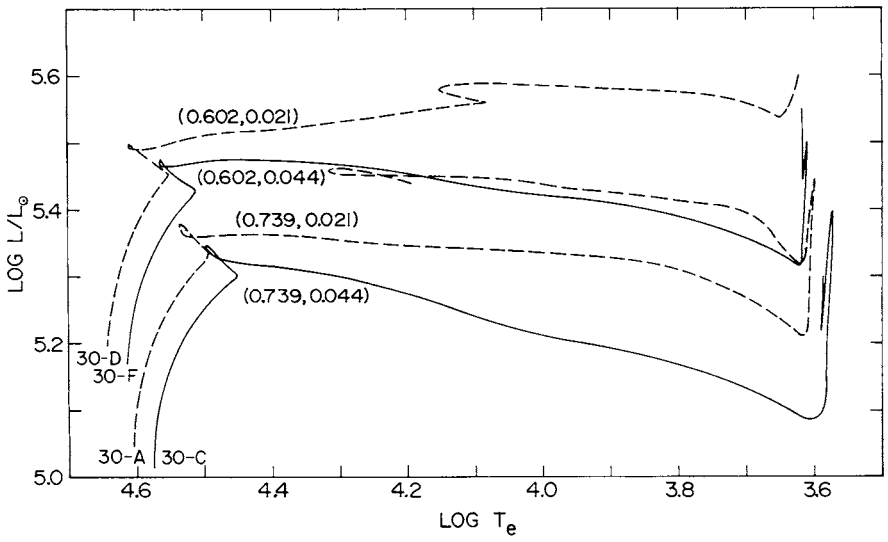

FIG. 6.—Theoretical evolutionary tracks in the H-R diagram for stars of 30 $M_\odot$. Tracks are labeled with (X_e, Z_e).

the outer convective envelope to penetrate to deeper levels than were attained by the models in Paper II. This promotes a blue loop, not found when semiconvection is not taken into account. When the star becomes a blue supergiant, convective instability breaks out anew in the hydrogen plateau that was formed earlier by the deep incursion of surface convection. When this convective instability reaches the inner edge of the hydrogen plateau, where the burning shell is located, a thin semiconvective zone is set up in the upper layers of the burning region. But the whole picture of evolution changes if the old 3α rate is adopted; in that case the blue loop never develops because the maximum depth of the outer convective envelope is too shallow. In fact, the occurrence of the blue loop in the original sequence seems to be very marginal. A rerun of the original sequence with different mass-zoning criteria was made, and gave a slightly shallower semiconvective zone (and hence a slightly shallower outer convective envelope); consequently, the blue loop never formed. In Ziołkowski's (1972) sequence with $(X_e, Z_e) = (0.70, 0.03)$ and no semiconvective mixing, a blue loop unexpectedly developed, because the convective envelope happened to be sufficiently deep.

For $(X_e, Z_e) = (0.739, 0.044)$ the high metals opacity maintains convective instability in the intermediate zone as the star moves across the H-R diagram, until the bottom of the red-supergiant branch is reached (see Fig. 8). But, before this point is attained,

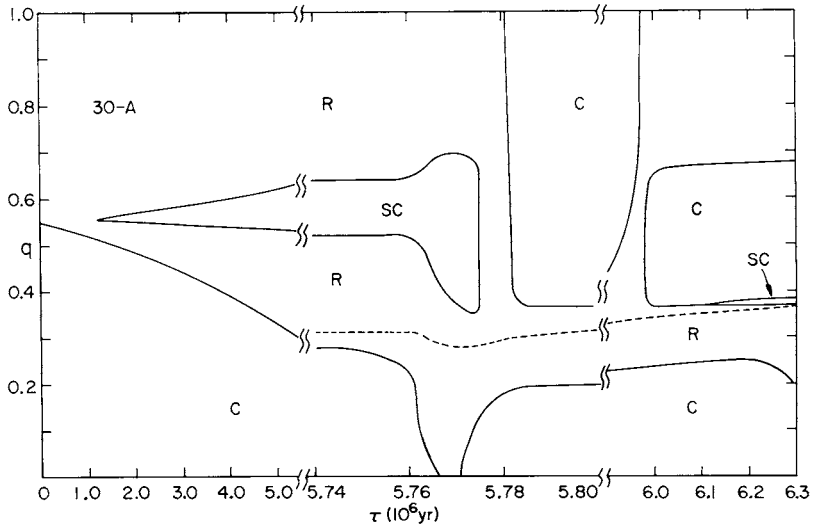

FIG. 7.—Evolution of the structural zones of a star of 30 $M_\odot$ with $(X_e, Z_e) = (0.739, 0.021)$. Coding is the same as in Fig. 2.

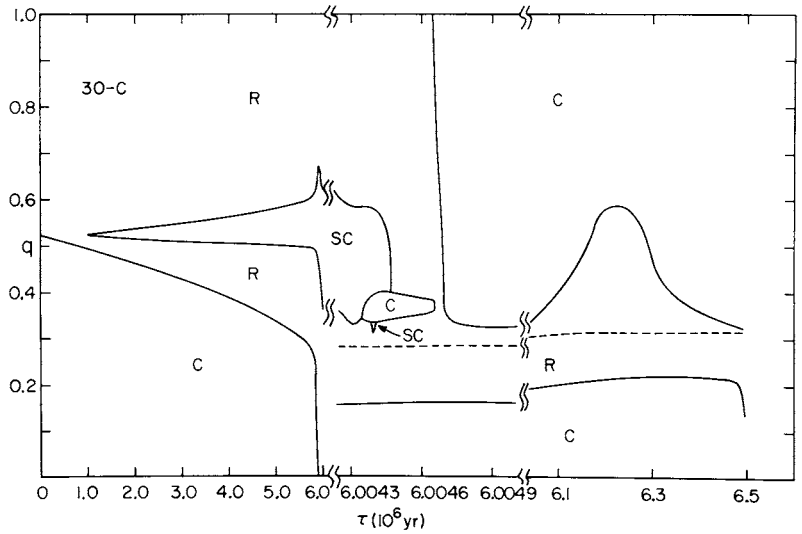

FIG. 8.—Evolution of the structural zones of a star of 30 $M_\odot$ with $(X_e, Z_e) = (0.739, 0.044)$. Coding is the same as in Fig. 2.

the lower part of the semiconvective zone becomes fully convective, at a time when $\log T_e = 3.75$. Shell burning is relatively weak, and the mass fraction of the hydrogen shell marches out only half as rapidly as in the sequence with smaller Z_e. The hydrogen shell and the base of the outer convective envelope (despite its depth) therefore remain well separated, and a blue loop on the H-R diagram never forms. The evolution of the hydrogen profile within the star is shown in Figure 9.

For $(X_e, Z_e) = (0.602, 0.021)$ the luminosity of the star is very bright because the core mass is large and because the interior opacity is low. One consequence of the high luminosity is that convective instability occurs over a considerable mass of the intermediate zone (see Fig. 10). So deep, in fact, lies the base of the semiconvective zone that the burning shell runs into it shortly after the stage of central hydrogen exhaustion, while the star is still a blue supergiant. However, the shell remains thermally stable despite its great thermal

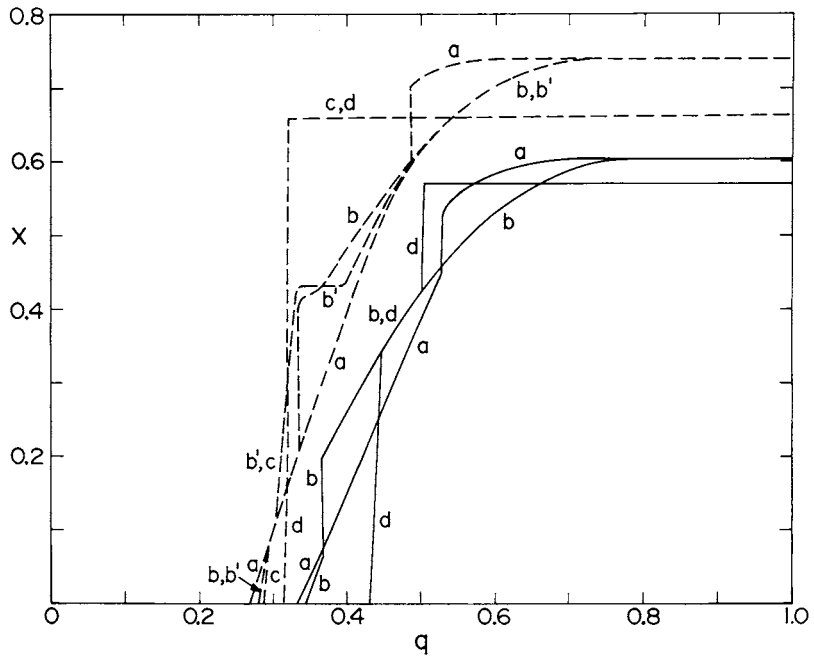

FIG. 9.—Hydrogen profiles for stellar models of 30 $M_\odot$ with $Z_e = 0.021$ (*solid lines*, sequence 30-D) and $Z_e = 0.044$ (*dashed lines*, sequence 30-C). Lettering index: *a*, end of core hydrogen burning; *b*, maximum extent of semiconvective zone; *b'*, maximum extent of fully convective intermediate zone; *c*, tip of the red-supergiant branch; and *d*, end of core helium burning.

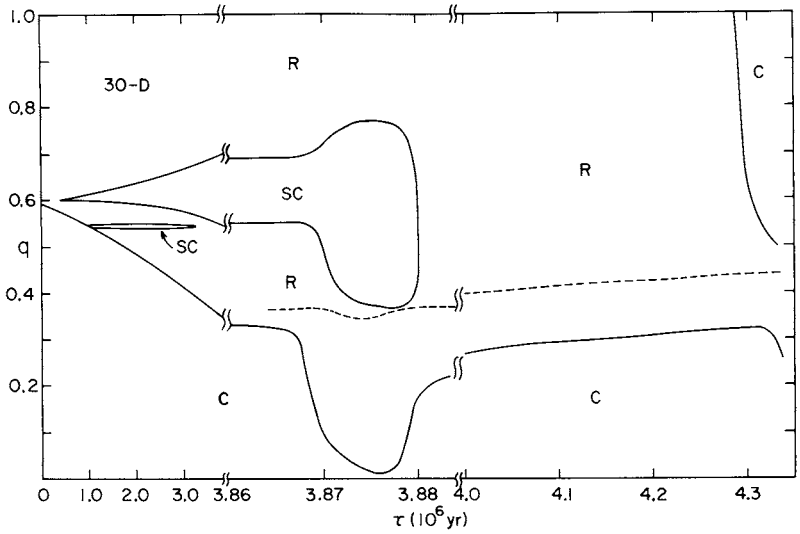

FIG. 10.—Evolution of the structural zones of a star of 30 $M_\odot$ with $(X_e, Z_e) = (0.602, 0.021)$. Coding is the same as in Fig. 2.

thickness. The hydrogen-helium discontinuity at the shell peak is sufficiently pronounced (see Fig. 9), and the envelope opacity is sufficiently low, that the envelope is quickly stabilized against further expansion, in accordance with the results of Paper I. These factors also ensure that the subsequent "blue hook" on the H-R diagram is small in extent. (Were the hydrogen jump through the shell greater, the leftward extension of the blue hook would be even shorter.) However, long before the blue hook begins, semiconvection has ceased (at $\log T_e = 4.42$), and is never reactivated even when the star commences its rapid movement across the Hertzsprung gap during the phase of core helium exhaustion (at $\log T_e = 3.85$).[2] The evolutionary track for the present case is particularly reminiscent of two earlier tracks in which electron scattering was specified to be the sole opacity source (Stothers 1966) or else the dominant opacity source, due to a very low adopted initial metals abundance (Trimble, Paczynski, and Zimmerman 1973).

For $(X_e, Z_e) = (0.602, 0.044)$ the semiconvective zone first disappears when $\log T_e = 4.27$, although it is partly reactivated when the star crosses the Hertzsprung gap (see Fig. 11). Nevertheless, the maximum extent of semiconvection is less for the present chemical composition than for the other three compositions, and consequently the semiconvective zone has less effect on the star's subsequent evolution. As in Paper II, the star remains a red supergiant throughout the phase of core helium burning, regardless of which nuclear reaction rates are adopted.

[2] Our sequences at 15 and 30 $M_\odot$ with $(X_e, Z_e) = (0.602, 0.021)$ did not develop a fully convective inward extension of the semiconvective zone. However, Robertson's (1972) sequence at 20 $M_\odot$ with nearly the same chemical composition, $(X_e, Z_e) = (0.617, 0.020)$, did. The reason for the discrepancy is uncertain, but Robertson used (1) somewhat larger opacities than we did and (2) an *assumed* form of the hydrogen dependence of the opacity law during the iterations for semiconvective mixing in his models; this assumed form, we have found in a special sequence computed for 20 $M_\odot$, induces a spurious fully convective zone.

IV. CONCLUSION

Semiconvective mixing according to the Ledoux criterion has been included in new evolutionary sequences of models for stars of 10, 15, and 30 $M_\odot$, with four different initial chemical compositions. With the exception of one sequence at 30 $M_\odot$, the new sequences confirm the important result of Papers I and II that models based on the Ledoux criterion first achieve full thermal stability, after central hydrogen exhaustion, in the red-supergiant configuration. With the adoption of the new 3α rate, a "blue loop" on the H-R diagram always ensues at 10 and 15 $M_\odot$, regardless of whether semiconvective mixing is included or ignored. At 10 $M_\odot$ semiconvection is almost nonexistent anyway, while at 15 $M_\odot$, although it is stronger, its effect is to induce only a slightly earlier and longer blue loop than was the case without it. But at 30 $M_\odot$ semiconvection covers most of the intermediate zone, and develops into full convection if X_e and Z_e are large. Moreover, at this mass, semiconvection provides the conditions necessary for an (otherwise nonexistent) blue loop, as long as Z_e is small and the new 3α rate is adopted. In fact, if X_e is also small, the star does not even achieve its first red-supergiant configuration until the *end* of core helium burning.

Semiconvection promotes a blue loop by raising the hydrogen content of the deep layers of the intermediate zone of varying hydrogen-helium content. The composition modifications there increase the opacity and lower the gradient of mean molecular weight; therefore surface convection during the red-supergiant phase extends down to layers closer to the hydrogen-burning shell. In general, the higher the stellar mass, the weaker is the shell burning, and so the less is the

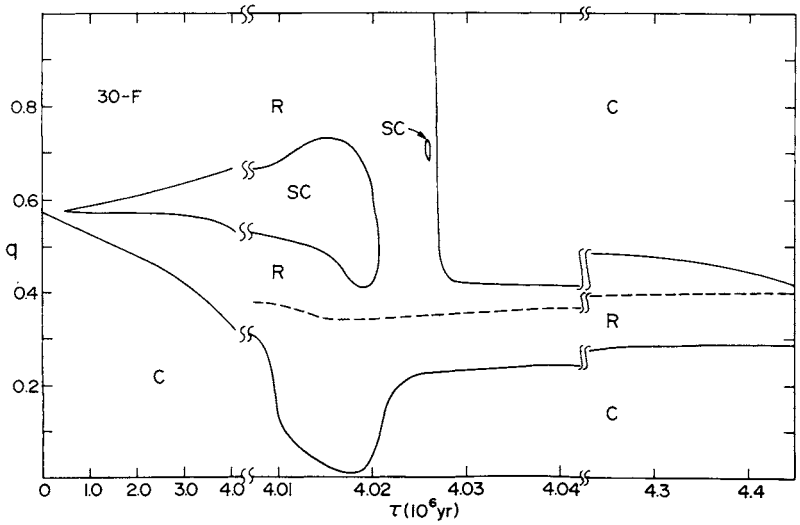

FIG. 11.—Evolution of the structural zones of a star of 30 $M_\odot$ with $(X_e, Z_e) = (0.602, 0.044)$. Coding is the same as in Fig. 2.

advance of the shell peak outward in mass fraction (Paper I). Consequently, there usually remains a significant chemically inhomogeneous region between the shell peak and the envelope base at higher masses; this keeps most of the 30 $M_\odot$ models red. The chemical discontinuity at the base of the semiconvective intermediate zone is usually too small to have any effect when the hydrogen-burning shell runs into it; such an encounter occurs only at 30 $M_\odot$, and has a large effect only when X_e and Z_e are low.

The rapid evolution of the star along the blue loop in the H-R diagram slows down when $\log T_e \approx 4.0$, 4.1, and 4.2, for masses of 10, 15, and 30 $M_\odot$, respectively. Thereafter, thermal stability of the envelope is restored, and core helium burning goes to completion (or near completion) in a stable blue-supergiant configuration. The slow blueward evolution of the star is eventually terminated, in all of the present sequences with a blue loop, when the shell peak fully merges with the base of the homogeneous envelope, although, in the sequences of Paper II, this merger occurred only for 15 $M_\odot$ with $Z_e = 0.044$.[3]

The main properties of the blue loop are collected in Table 3, and include properties determined in Paper II as well as a few available results from other sources. Notice that a diagonal "zone of occupation" for blue supergiants is predicted to exist on the H-R diagram; its width is approximately $\Delta \log T_e \approx 0.15$ at all luminosities, and its mean color is bluer at brighter luminosities. This prediction is in rough agreement with the observed distribution of early-type supergiants on the H-R diagram (Humphreys 1970; Stothers 1972), although a detailed comparison with observations must await further investigation of physical effects in the models.

[3] That an encounter between the hydrogen-burning shell and an overlying hydrogen plateau is not necessary to initiate or terminate a blue loop has also been demonstrated for massive stars by Murai (1974).

The predicted blue-to-red ratio for supergiants is more problematical. Observationally, it increases with stellar mass. But our *formal* results for various masses and initial chemical compositions are remarkably uniform. Indeed, we always seem to obtain $\tau_b/\tau_{He} = 0.5 \pm 0.2$ if a blue loop forms at all. However, the maximum convective-envelope depth on the red-supergiant branch is so dependent on opacity and assumptions about convective overshooting that it could be deeper than we and others have determined, and therefore it could perhaps induce a blue loop at a much earlier stage of core helium burning.[4] This greater depth could also affect, to a more limited extent, the maximum effective temperature attained at the tip of the blue loop.

On the other hand, when the Schwarzschild criterion is adopted for the definition of convective instability and for the state of convective neutrality that is attained in semiconvective layers, the star usually does

[4] One example of an early-developing loop is currently available: the 20 $M_\odot$ sequence of Chiosi and Summa (1970) has $\tau_b/\tau_{He} = 0.8$; otherwise, it fits in satisfactorily with our grid of model sequences. Ziołkowski (1972) has also discussed the possibility of an early-developing loop.

TABLE 3

PARAMETERS OF THE BLUE LOOP

$M/M_\odot$	Semiconvection	$\log T_e$ (b/y)	$\log T_e$ (tip)	τ_b/τ_{He}
10	Yes	~4.0	4.15 ± 0.03	0.6 ± 0.1
	No	~4.0	4.15 ± 0.03	0.6 ± 0.1
15	Yes	~4.1	4.26 ± 0.03	0.5 ± 0.1
	No	~4.1	4.22 ± 0.03	0.5 ± 0.2
30	Yes*	~4.2	4.32:	0.6:
	No†	~4.2	4.38:	0.5:

* Based on one sequence.

† Based on one sequence due to Ziołkowski 1972. All our sequences remained red.

not evolve into a red supergiant until near the end of core helium burning (Stothers and Chin 1975). It is found that the predicted blue-to-red ratio at first increases with stellar mass, approximately as is observed. However, at the higher masses, the predicted ratio then starts to decrease, and the effective temperature during the slow blue phase of evolution is mostly cooler than observed. Thus, further theoretical work is needed on stellar models constructed with both schemes of semiconvection before the observational data can be used to decide between them. We are currently engaged in the necessary additional studies.

REFERENCES

Austin, S. M., Trentelman, G. F., and Kashy, E. 1971, *Ap. J. (Letters)*, **163**, L79.
Chiosi, C., and Summa, C. 1970, *Ap. and Space Sci.*, **8**, 478.
Clayton, D. D. 1968, *Principles of Stellar Evolution and Nucleosynthesis* (New York: McGraw-Hill).
Humphreys, R. M. 1970, *Ap. Letters*, **6**, 1.
Ledoux, P. 1947, *Ap. J.*, **105**, 305.
Murai, T. 1974, *Pub. Astr. Soc. Japan*, **26**, 323.
Paczynski, B. 1970, *Acta Astr.*, **20**, 195.
Percy, J. R. 1970, *Ap. J.*, **159**, 177.
Robertson, J. W. 1972, *Ap. J.*, **177**, 473.
Sackmann, J. 1971, in *Colloquium on Supergiant Stars*, ed. M. Hack (Trieste: Trieste Astronomical Observatory), p. 323.
———. 1974, *Astr. and Ap.*, **34**, 241.
Sakashita, S., and Hayashi, C. 1961, *Progr. Theoret. Phys. (Kyoto)*, **26**, 942.
Sakashita, S., Ono, Y., and Hayashi, C. 1959, *Progr. Theoret. Phys. (Kyoto)*, **21**, 315.
Schwarzschild, M., and Härm, R. 1958, *Ap. J.*, **128**, 348.
Simpson, E. E. 1971, *Ap. J.*, **165**, 295.
Sreenivasan, S. R., and Ziebarth, K. E. 1974, *Ap. and Space Sci.*, **30**, 57.
Stothers, R. 1966, *Ap. J.*, **143**, 91.
———. 1970, *M.N.R.A.S.*, **151**, 65.
———. 1972, *Ap. J.*, **175**, 431.
Stothers, R., and Chin, C.-w. 1968, *Ap. J.*, **152**, 225 (Paper I).
———. 1973, *ibid.*, **179**, 555 (Paper II).
———. 1975, in preparation.
Trimble, V., Paczynski, B., and Zimmerman, B. A. 1973, *Astr. and Ap.*, **25**, 35.
Varshavsky, V. I. 1972, *Nauch. Inform.*, No. 21, p. 25.
———. 1973, *Soviet Astr.—AJ*, **16**, 861.
Varshavsky, V. I., and Tutukov, A. V. 1973, *Nauch. Inform.*, No. 26, p. 35.
Ziołkowski, J. 1972, *Acta Astr.*, **22**, 327.

CHAO-WEN CHIN and RICHARD STOTHERS: Institute for Space Studies, Goddard Space Flight Center, NASA, 2880 Broadway, New York, NY 10025